Resource

Cell Reports

The Hsp70 Chaperone System Stabilizes a Thermo-sensitive Subproteome in *E. coli*

Graphical Abstract

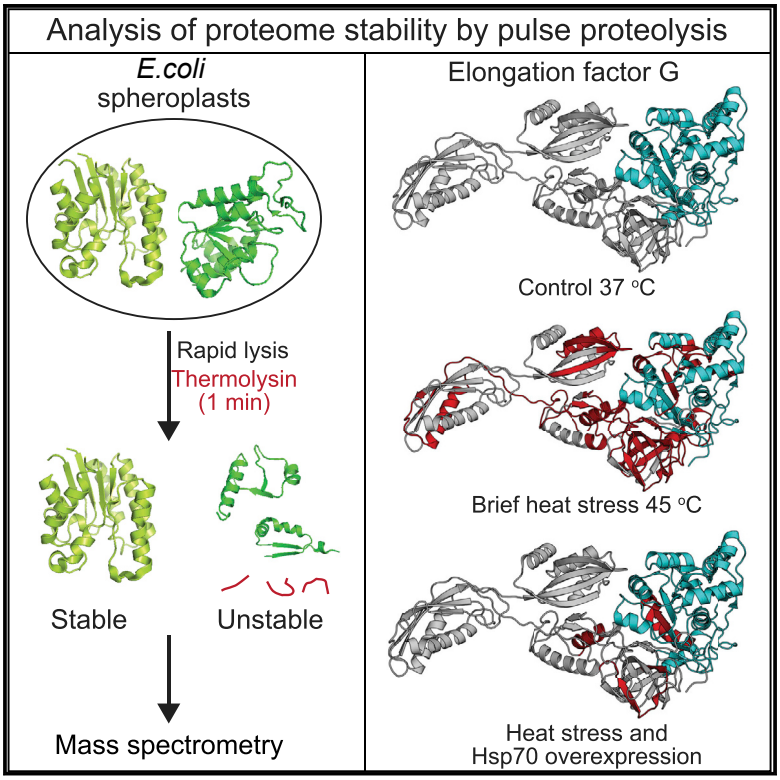

Highlights

- Acute heat stress causes unfolding of a thermo-sensitive subproteome in *E. coli*
- DnaK (Hsp70) markedly stabilizes most thermo-sensitive proteins
- Numerous essential ribosomal proteins are conformationally stabilized by DnaK
- Other DnaK-stabilized proteins tend to be large, multi-domain, and hetero-oligomeric

Authors

Liang Zhao, Giulia Vecchi, Michele Vendruscolo, Roman Körner, Manajit Hayer-Hartl, F. Ulrich Hartl

Correspondence

mhartl@biochem.mpg.de (M.H.-H.), uhartl@biochem.mpg.de (F.U.H.)

In Brief

Molecular chaperones function in maintaining protein homeostasis. Zhao et al. analyze proteome stability in *Escherichia coli* using pulse proteolysis and mass spectrometry. Numerous ribosomal proteins as well as large multi-domain proteins unfold upon heat stress. Overexpression of the DnaK (Hsp70) chaperone system markedly stabilizes thermo-sensitive proteins in their folded conformations.

Zhao et al., 2019, Cell Reports *28*, 1335–1345
July 30, 2019
https://doi.org/10.1016/j.celrep.2019.06.081

CellPress

Cell Reports
Resource

The Hsp70 Chaperone System Stabilizes a Thermo-sensitive Subproteome in *E. coli*

Liang Zhao,[1] Giulia Vecchi,[2] Michele Vendruscolo,[2] Roman Körner,[1] Manajit Hayer-Hartl,[3,*] and F. Ulrich Hartl[1,4,*]
[1]Department of Cellular Biochemistry, Group Cellular Biochemistry, Max Planck Institute of Biochemistry, Am Klopferspitz 18, Martinsried 82152, Germany
[2]Centre of Misfolding Diseases, Department of Chemistry, University of Cambridge, Lensfield Road, Cambridge CB2 1EW, UK
[3]Department of Cellular Biochemistry, Group Chaperonin-assisted Protein Folding, Max Planck Institute of Biochemistry, Am Klopferspitz 18, Martinsried 82152, Germany
[4]Lead Contact
*Correspondence: mhartl@biochem.mpg.de (M.H.-H.), uhartl@biochem.mpg.de (F.U.H.)
https://doi.org/10.1016/j.celrep.2019.06.081

SUMMARY

Stress-inducible molecular chaperones have essential roles in maintaining protein homeostasis, but the extent to which they affect overall proteome stability remains unclear. Here, we analyze the effects of the DnaK (Hsp70) system on protein stability in *Escherichia coli* using pulse proteolysis combined with quantitative proteomics. We quantify ~1,500 soluble proteins and find ~500 of these to be protease sensitive under normal growth conditions, indicating a high prevalence of conformationally dynamic proteins, forming a metastable subproteome. Acute heat stress results in the unfolding of an additional ~200 proteins, reflected in the exposure of otherwise buried hydrophobic regions. Overexpression of the DnaK chaperone system markedly stabilizes numerous thermo-sensitive proteins, including multiple ribosomal proteins and large, hetero-oligomeric proteins containing the evolutionarily ancient c.37 fold (P loop nucleoside triphosphate hydrolases). Thus, the Hsp70 system, in addition to its known chaperone functions, has a remarkable capacity to stabilize proteins in their folded states under denaturing stress conditions.

INTRODUCTION

Native proteins are structurally dynamic (Gershenson et al., 2014), and thus the cellular proteome requires constant conformational surveillance by an integrated network of chaperones and protein degradation machineries to maintain a functional state (Balch et al., 2008; Balchin et al., 2016; Wolff et al., 2014). External and endogenous stress conditions may cause proteins to undergo partial or complete unfolding events, which can result in aberrant interactions and the formation of potentially toxic aggregates. Molecular chaperones prevent such off-pathway reactions (Balchin et al., 2016; Clerico et al., 2015; Frydman, 2001), but the extent to which the proteome is conformationally destabilized under stress conditions and the protective capacities of chaperone systems have not yet been analyzed in detail.

The highly conserved Hsp70 chaperones serve as a central hub of the protein homeostasis system (Bhandari and Houry, 2015; Clerico et al., 2015; Mayer and Bukau, 2005; Mayer and Gierasch, 2019). DnaK, the main bacterial Hsp70, functions by binding and releasing, in an ATP-dependent manner, hydrophobic polypeptide segments that are exposed in non-native proteins (Clerico et al., 2015; Mayer, 2013; Rüdiger et al., 1997). DnaK functionally cooperates with the Hsp40 co-chaperone DnaJ and the nucleotide exchange factor GrpE. During *de novo* protein folding, DnaK functions downstream of the ribosome-binding chaperone trigger factor (TF) (Deuerling et al., 1999; Teter et al., 1999). Moreover, DnaK is strongly upregulated under heat stress (HS) to counteract protein aggregation (Mogk et al., 1999). Approximately 700 newly synthesized and preexisting proteins, which make up ~25% of the cytosolic proteome, have been shown to interact with DnaK (Calloni et al., 2012).

Pulse proteolysis (PP) has recently emerged as a powerful method to study, at the proteome level and in a quantitative manner, the factors that affect protein stability. As under steady-state conditions proteins are in equilibrium between folded and unfolded states, local or overall unfolding events frequently take place. PP can quantify non-native conformations by taking advantage of the fact that unfolded proteins are more susceptible to proteolysis than folded proteins (Park et al., 2007; Park and Marqusee, 2005). Folded states remain largely intact, as the fraction of protein that unfolds during the short protease pulse is small. In conjunction with mass spectrometry (MS), PP has been used to study protein folding or conformational changes in complex samples (Adhikari and Fitzgerald, 2014; Feng et al., 2014; Leuenberger et al., 2017; Tran et al., 2014).

Here, we performed PP with thermolysin and quantitative proteomics on amino acid isotope-labeled *Escherichia coli* (PP-SILAC [stable isotope labeling with amino acids in cell culture]) to analyze the effects of the DnaK chaperone system on proteome stability. We found numerous ribosomal proteins as well as large, multi-domain proteins to be susceptible to HS-induced unfolding, with protease cleavage occurring in hydrophobic sequence regions that are normally buried in the native state. In particular, proteins with domains of the evolutionarily ancient c.37 fold (P loop nucleoside triphosphate hydrolases) are significantly enriched in the thermo-sensitive subproteome.

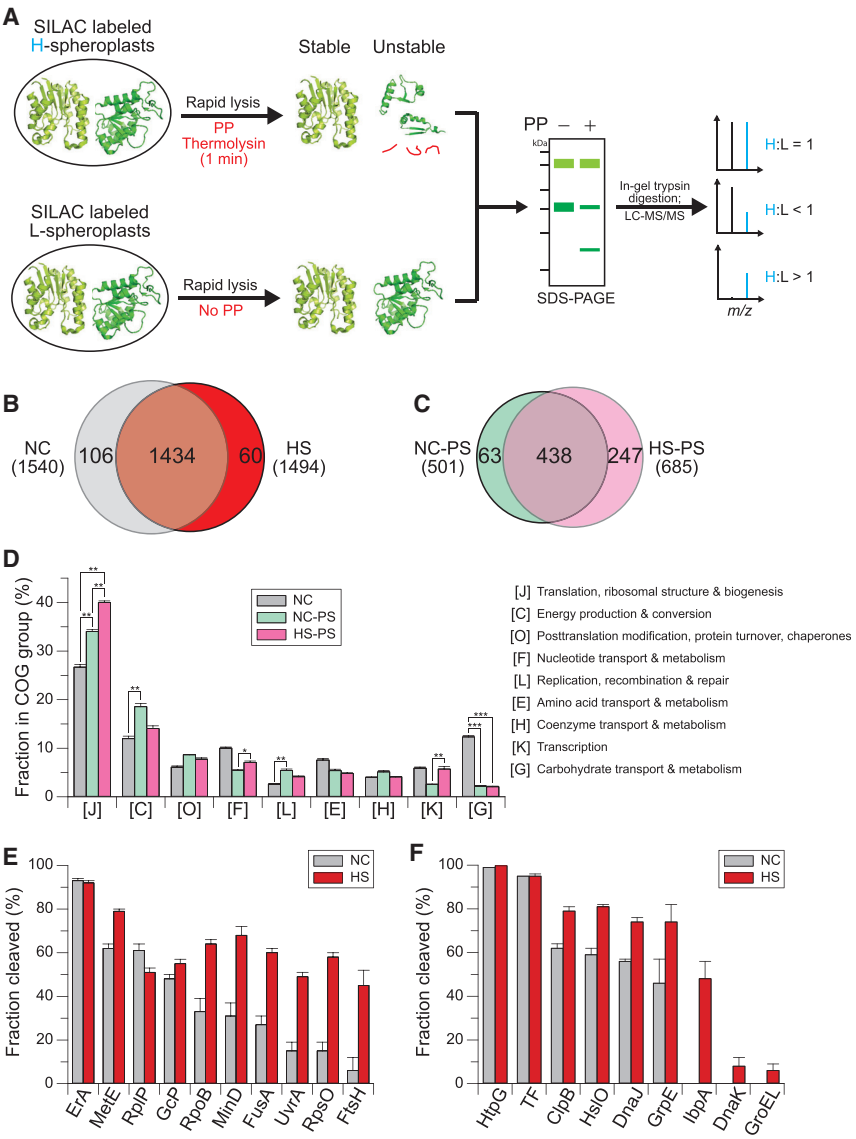

Figure 1. PP Analysis at 37°C and upon HS

(A) Schematic representation of the PP-SILAC workflow for the analysis of protease-sensitive (PS) fractions of proteins. SILAC-labeled *E. coli* cells (spheroplasts) are lysed with or without PP, mixed, and separated by SDS-PAGE. Quantitative proteomic analysis of SILAC ratios of tryptic peptides in gel slices enables the quantification of cleaved protein fractions. Stable proteins are in light green and unstable (protease sensitive) proteins in dark green.

(B and C) Venn diagrams of sets of proteins quantified at a NC of 37°C and after a 15-min exposure of spheroplasts to HS at 45°C (B) and of PS proteins identified under these conditions (NC-PS and HS-PS, respectively) (C). See Tables S2A and S2B.

(D) The most abundant COG of proteins categories in the sets of NC-PS and HS-PS proteins compared to lysate control (NC). The values were normalized to the total number of PS proteins across all of the COG categories, for either the NC or the HS condition. The error bars represent means ± SEMs (n = 3). p values are based on paired t test (two-tailed): *p ≤ 0.05, **p ≤ 0.01, and ***p ≤ 0.001.

(E and F) Protease sensitivity of selected proteins (E) and chaperone proteins (F) in NC (Table S2A) and HS (Table S2B). The fractions cleaved by PP are indicated. The values represent means ± SEMs (n = 3).

Overexpression of the DnaK chaperone machinery before heat treatment markedly stabilized numerous thermo-sensitive proteins in their folded conformations. Hsp70 may carry out this action by reversing kinetically trapped misfolded states, thereby shifting the equilibrium of folding intermediates toward native states.

RESULTS

PP Workflow

To analyze the conformational stability of proteins, we labeled MC4100 *E. coli* cells with heavy (H) arginine and lysine isotopes at 37°C and prepared live spheroplasts. PP was performed with the metallo-proteinase thermolysin for 1 min during rapid hypo-osmotic cell lysis and efficiently stopped with EDTA (Figure 1A), as demonstrated with the intrinsically unstructured α-synuclein (α-Syn) as the substrate (Figure S1A). Thermolysin has a broad cleavage specificity with a preference for hydrophobic amino acids that are normally buried in the core of folded proteins (Tables S1A and S1B). Unlabeled spheroplasts (light, L) were treated identically but received no protease. Equal amounts of lysate from L- and H-spheroplasts were mixed and proteins were separated by SDS-PAGE, followed by in-gel digestion with trypsin and liquid chromatography-tandem MS (LC-MS/MS) analysis (Figure 1A). The tryptic peptides of a stable protein will show an H:L isotope ratio of 1, whereas a ratio <1 indicates that the protein is sensitive to PP. Stable proteolytic fragments (domains) generated by PP would show H:L ratios >1 (Figure 1A). This analysis allows quantification of the extent of cleavage, and thus of protein stability. Note that the steady-state concentration of newly synthesized (presumably not yet folded and/or assembled) proteins in exponentially growing *E. coli* cells is ≤1.0% of the total and is expected to be even lower in spheroplasts (see STAR Methods). Thus, the PP-SILAC method used in this study essentially measures the stability of preexistent proteins.

We validated the PP-SILAC workflow using the unstructured α-Syn as a positive control and the stably folded maltose binding protein (MBP) (Park et al., 2007) as a negative control. The proteins were added in isotope-labeled (H) form to the spheroplast suspension, followed by cell lysis and PP for 1 min at 37°C. After the inhibition of proteolysis, equal amounts of unlabeled (L) α-Syn and MBP were added. The concentration of thermolysin (~120 μg/mL) was adjusted such that α-Syn was efficiently

degraded upon PP (H:L <0.1 for all of the peptides identified; Figure S1B), whereas MBP was resistant (H:L >0.9 for all of the peptides identified; Figure S1C). In the case of α-Syn, the peptides generated by thermolysin partially or completely overlapped with tryptic peptides (Figure S1B), which is consistent with the unstructured nature of α-Syn. MBP was stable during PP both at 37°C and upon heat treatment (15 min at 45°C) (Figure S1D). In summary, PP-SILAC reliably distinguishes between stably folded and conformationally heterogeneous proteins.

PP under Normal and HS Conditions

We first performed PP-SILAC under normal growth conditions (NCs) at 37°C (henceforth designated NC) and quantified 1,540 proteins in at least 2 of 3 biological replicates with high reproducibility (Figures 1B and S2A; Table S2A). These proteins were mostly localized to the cytosol (Figure S2B), and their cellular abundance ranged from <50 copies per cell for the putative lipoprotein AcfD homolog (YghJ) to ~70,000 copies for the 30S ribosomal protein S16 (RpsP) (Schmidt et al., 2016; Table S2A). Based on control experiments, the significant ($p < 0.01$) cutoff value for the H:L ratio that defines a protein as protease sensitive (PS) was determined to be <0.61—in other words, 39% of the total of a specific protein must be degraded (Figure S2C; STAR Methods). Applying this cutoff (in at least 2 repeats), we found 501 proteins to be significantly degraded (NC-PS), corresponding to ~25% of the quantified proteins by mass (Figure 1C; Table S2A; STAR Methods). Thus, a substantial fraction of *E. coli* proteins are sensitive to PP at NC, suggesting that they are conformationally dynamic and that they expose protease cleavage sites in flexible regions.

To determine protein stabilities upon acute HS, we shifted spheroplasts from 37°C to 45°C for 15 min, followed by PP at 37°C (see STAR Methods). We reproducibly quantified 1,494 proteins (HS) (Figure S2D; Table S2B) showing almost complete overlap with the 1,540 proteins quantified at NC (Figure 1B). A total of 685 proteins were significantly degraded by PP upon HS (HS-PS), corresponding to ~33% of the quantified proteins by mass (Table S2B; STAR Methods). These HS-PS proteins largely overlap with the set of NC-PS proteins (87%) and include 247 proteins that were not identified as NC-PS (Figure 1C; Table S2B). A total of 188 proteins were significantly more protease sensitive upon HS compared to NC and are thus defined as thermo-sensitive (Table S2C). Note that the brief heat treatment caused only a moderate upregulation of the major stress-inducible chaperone proteins DnaK, HtpG (both ~1.7-fold), and GroEL (~1.2-fold) (Table S2D; STAR Methods). Thus, it is unlikely that protein stabilities were substantially modulated by the cellular stress response in these experiments. Fractionation of cell lysates showed that only ~0.8% of the total protein by mass aggregated, which is consistent with a previous report (Winkler et al., 2010; Table S2E; STAR Methods), indicating that protein aggregation did not interfere with the PP analysis.

Functions of Protease-Sensitive Proteins

Gene Ontology (Clusters of Orthologous Groups [COG] database) analysis (Tatusov et al., 2000) showed that NC-PS and HS-PS proteins are preferentially involved in the cellular processes of protein biogenesis (class J) and energy production (class C), with enzymes of carbohydrate metabolism (class G) being deenriched (Figure 1D). We found that NC-PS proteins have significantly more interactors than protease-stable proteins, indicating higher connectivity in the functional networks (Figure S2E), which is consistent with the notion that proteins having multiple interactors tend to be structurally more dynamic (Bardwell and Jakob, 2012). Numerous proteins of the 30S and 50S ribosome (23 of 49 quantified ribosomal proteins) and many nucleotide-binding proteins were PP sensitive at NC (Figure 1E; Table S2A), which is indicative of a high degree of structural flexibility of these protein groups. For example, the guanosine triphosphatase (GTPase) ErA was almost completely cleaved, while the putative tRNA threonylcarbamoyladenosine biosynthesis protein GcP was ~50% degraded (Figure 1E). Many moderately protease-sensitive (PS) or largely stable proteins were destabilized upon HS, including the septum site-determining protein MinD, the elongation factor G (FusA), the nucleotide excision repair protein excinuclease ABC (subunit A) (UvrA), and the ATP-dependent zinc metalloprotease FtsH (Figure 1E). These findings are consistent with HS resulting in a decrease in protein biogenesis and slow growth (Chen et al., 2017). Several molecular chaperones such as HtpG (Hsp90) and TF were already completely protease sensitive (95%–100%) at NC, and thus any further destabilization upon HS could not be measured (Figure 1F). ClpB, HslO, DnaJ, and GrpE, while conformationally dynamic at NC (50%–60% cleaved), were further destabilized upon HS (Figure 1F). The small heat shock protein IbpA was specifically thermo-sensitive, suggesting that an order-to-disorder transition upon HS may play a role in its activation for client binding (Bardwell and Jakob, 2012; Tompa and Kovacs, 2010). In contrast, the Hsp70 DnaK and the chaperonin GroEL were highly protease stable (Figure 1F). Unlike trypsin (Buchberger et al., 1995), thermolysin is inefficient in cleaving the linker between the ATPase and peptide-binding domains of DnaK, as demonstrated with purified DnaK (Figure S2F).

Effects of Overexpressing the DnaK System on Protein Stability

DnaK, together with its co-chaperone DnaJ and its nucleotide exchange factor GrpE, have a central role in the cytosolic chaperone network (Calloni et al., 2012; Mayer and Bukau, 2005; Mayer and Gierasch, 2019). To gain insight into the effect of the DnaK/DnaJ/GrpE (KJE) machinery on the overall proteome stability, we overexpressed these proteins from an isopropyl-β-D-thiogalactopyranosid (IPTG)-inducible plasmid for ~1 h at NC. Cells were then further incubated at NC (NC/KJE) or exposed to HS (HS/KJE), followed by PP at 37°C. The levels of KJE increased ~6- to 11-fold in NC/KJE cells compared to NC cells, which are ~2-fold higher than the levels of KJE upon prolonged HS (Figure S3A; Table S3A). Other cytosolic chaperones and stress-inducible proteases remained unchanged upon KJE overexpression, in contrast to prolonged HS (Figure S3A). Thus, overexpression of KJE allowed us to specifically assess the potential of this chaperone system in modulating protein stability.

We quantified 1,564 proteins in NC/KJE and 1,469 proteins in HS/KJE cells by PP-SILAC, and identified 454 and 594 PS proteins, respectively (NC/KJE-PS and HS/KJE-PS) (Figures 2A, 2B, S3B, and S3C; Tables S3B and S3C). These proteins overlap

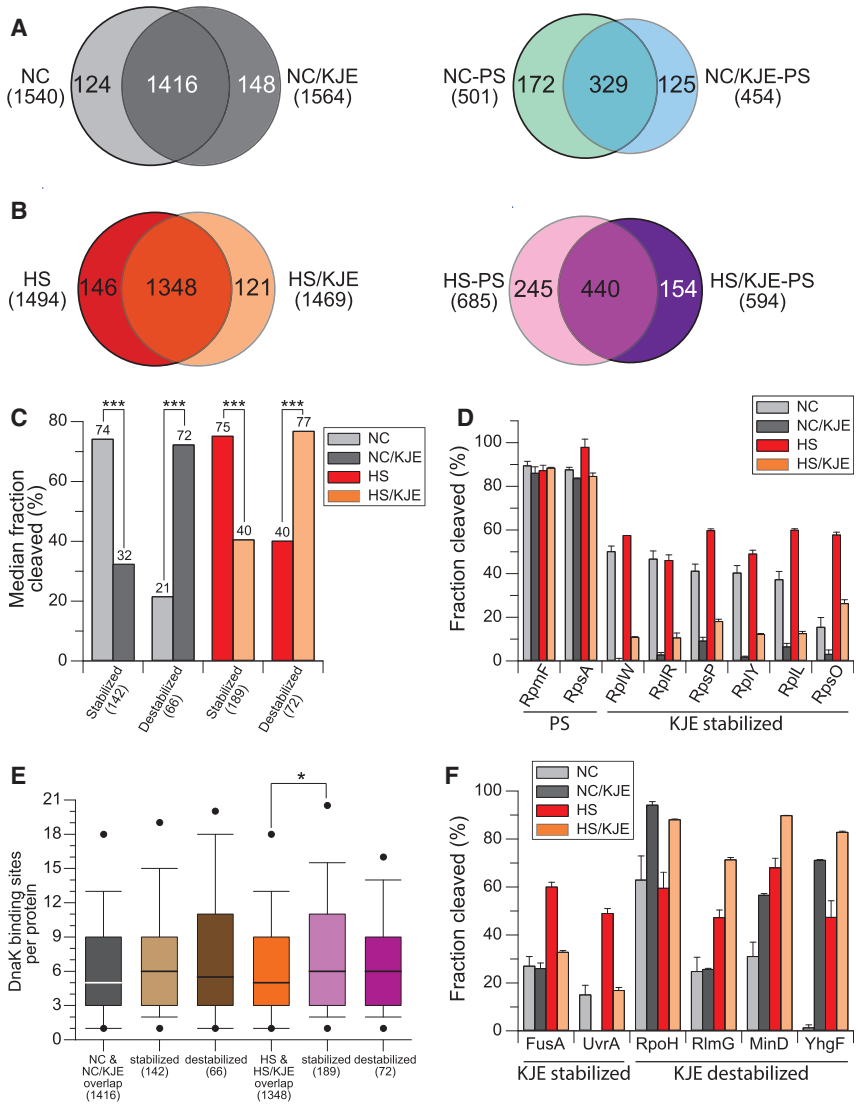

Figure 2. Effects of the DnaK Chaperone System on Protein Stability

(A and B) Venn diagrams of proteins analyzed in NC (A) and HS (B). Proteins are quantified in cells with overexpression of the DnaK chaperone system (NC/KJE and HS/KJE) and without KJE overexpression (NC and HS) on the left, and PS proteins are identified under these conditions (NC-PS and NC/KJE-PS; HS-PS and HS/KJE-PS) on the right (see Tables S2A, S2B, S3B, and S3C).

(C) Stabilization and destabilization of proteins upon KJE overexpression in NC and HS. Median fractions cleaved of proteins upon PP are indicated. p value based on the Mann-Whitney test: ***$p \leq 0.001$. The numbers of proteins analyzed are indicated in parentheses.

(D) Effect of KJE overexpression on the stability of ribosomal proteins. Median fractions cleaved upon PP are indicated. The error bars represent SEMs (n = 3). PS denotes ribosomal proteins not stabilized by KJE.

(E) Number of predicted DnaK binding sites in proteins stabilized and in proteins destabilized by KJE overexpression at NC and HS. The proteins quantified in both NC and NC/KJE cells or HS and HS/KJE are analyzed as reference. The horizontal lines in the boxplots indicate the median; whisker caps and circles indicate the 10th–90th and 5th–95th percentiles, respectively. p value based on the Mann-Whitney test: *$p \leq 0.05$. The numbers of proteins analyzed are indicated in parentheses.

(F) Examples of proteins stabilized and destabilized by KJE overexpression in NC and HS. The median fractions cleaved upon PP are indicated. The error bars represent means ± SEMs (n = 3).

extensively with the set of 501 NC-PS proteins and 685 HS-PS proteins, respectively (Figures 2A and 2B). The NC/KJE-PS proteins amount to ~20% of total quantified proteins and the HS/KJE-PS proteins to ~24% by mass, compared to ~25% and ~33% without KJE overexpression. Overexpression of KJE stabilized 142 NC-PS proteins (p = 0.003) and 189 HS-PS proteins (p = 0.002), with an overlap of 99 proteins (Tables S3D and S3F). The median cleaved fraction of these proteins shifted from ~75% to ~30%–40% (Figure 2C). Thus, the DnaK chaperone machinery strongly stabilizes the proteome both at NC and upon HS.

The KJE-stabilized proteins are preferentially ribosomal proteins, RNA-binding proteins and GTP-binding proteins (Figure S3D; Tables S3D and S3F). Only 2 of 49 quantified ribosomal proteins were protease sensitive in NC/KJE and 6 in HS/KJE cells (Figures 2D and S3E; Tables S2A and S3B), compared to 23 (NC) and 31 proteins (HS) without KJE overexpression (Figure S3E). These abundant proteins are highly conserved, with 19 of the 31 KJE stabilized ribosomal proteins being essential. While this result is consistent with a proposed role of DnaK in ribosome biogenesis (René and Alix, 2011), the extent of cleavage observed for several ribosomal proteins (fraction cleaved ≥50%) and the almost complete stabilization afforded by KJE (Figure 2D) indicate that the chaperones interact with assembled ribosomes, presumably maintaining functionality upon HS. In support of this notion, sucrose density gradient analysis of cell lysates showed that ribosomes did not dissociate upon brief HS (Figure S3F). Many of the KJE stabilized proteins (142 in NC and 189 in HS) are known DnaK interactors (Calloni et al., 2012; Tables S3D and S3F). These proteins have more predicted DnaK binding sites compared to the control set, as is particularly apparent for the proteins stabilized upon HS (Figure 2E). For example, the proteins FusA and UvrA (Figure 1E) were markedly stabilized by KJE, essentially regaining their stability at NC (Figure 2F).

KJE overexpression also destabilized a small group of ~70 proteins ($p \leq 0.003$), both in NC and upon HS (Figure 2C; Tables S3E and S3G). Their median protease-cleaved fraction shifted from 21% to 72% in NC/KJE and from 40% to 77% in HS/KJE cells (Figure 2C). These proteins also tend to contain more than average DnaK binding sites (Figure 2E). They function in transcription, DNA replication, and nitrogen biosynthetic processes

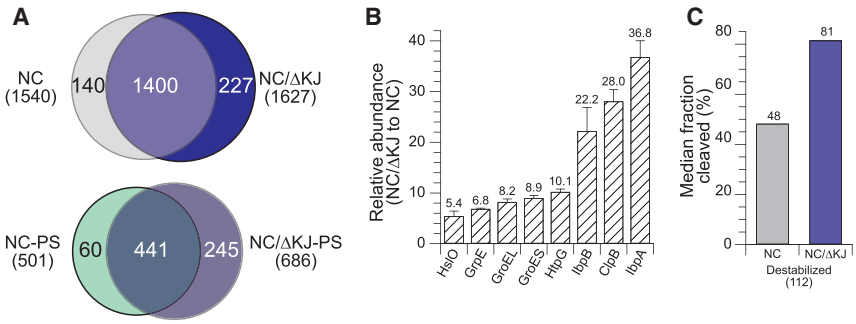

Figure 3. Effects of DnaK/DnaJ Deletion on Protein Stability

(A) Venn diagrams of proteins quantified and of PS proteins under normal conditions (NC) and in DnaK/DnaJ deleted cells (NC/ΔKJ) (see Tables S2A and S4A).

(B) Abundance change of chaperone proteins in ΔKJ cells compared to NC. The average fold changes are indicated. The error bars represent SEMs (n = 3).

(C) Destabilization of proteins in ΔKJ cells. The median fractions cleaved of the set of 112 proteins destabilized in ΔKJ cells compared to NC cells are indicated (see Table S4D).

(Figure S3G), including 15–18 essential proteins (Tables S3E and S3G). Notably, the heat shock regulator RpoH (σ^{32}), which is intrinsically unstable, was further destabilized by KJE (Figure 2F), as previously observed *in vitro* (Rodriguez et al., 2008). The cellular abundance of RpoH remained unchanged upon KJE overexpression, probably due to an ~93% depletion in the KJE cells of FtsH, the protease responsible for RpoH degradation (Arsène et al., 2000; Table S3A). MinD, another known DnaK interactor (Calloni et al., 2012), as well as the ribosomal methyltransferase RlmG and the RNA-binding protein YhgF were also destabilized (Figure 2F). Thus, the DnaK system apparently shifts the folding equilibrium of these proteins to unfolded states.

These results indicate that the DnaK chaperone machinery has opposing effects on protein stability. While numerous proteins are conformationally stabilized, including a large set of ribosomal proteins, a smaller subset of proteins is destabilized. For some proteins, DnaK-mediated destabilization may serve a regulatory function, as in the case of RpoH (Rodriguez et al., 2008).

Loss of DnaK Destabilizes the Proteome

Deletion of DnaK (together with DnaJ) results in the slow growth of *E. coli* and the inability to grow under HS (Bukau and Walker, 1989; Genevaux et al., 2004). The ribosome binding TF partially replaces the function of DnaK/DnaJ in folding newly synthesized proteins (Deuerling et al., 1999; Genevaux et al., 2004; Teter et al., 1999). To assess the possible role of the DnaK chaperone system in maintaining protein stability at the normal growth temperature of 37°C, we performed PP-SILAC in Δ*dnaKdnaJ* (ΔKJ) cells. We quantified 1,627 proteins that largely overlap with the set of 1,540 NC proteins and found 686 proteins to be PP sensitive (NC/ΔKJ-PS) (Figures 3A and S4; Table S4A). The NC/ΔKJ-PS proteins show a ~90% overlap with the set of NC-PS proteins and include an additional 245 PS proteins (Figure 3A). Approximately 33% of all proteins by mass were sensitive to PP in ΔKJ cells, compared to ~25% in NC cells. Exposure of ΔKJ cells to HS (15 min 45°C) had only a moderate additional destabilizing effect, with only 6 proteins being identified as thermo-sensitive (Table S4B). This relative protection against acute stress may be attributed to a strong constitutive upregulation of other chaperones in ΔKJ cells (Figure 3B; Table S4C), which is consistent with an ~3.7-fold increase in the abundance of RpoH (Table S4C). Conversely, the destabilization of proteins in ΔKJ cells at NC may be caused by not only the loss of DnaK but also a condition of chronic stress with chaperone deregulation.

Of the 1,400 proteins quantified in both NC and NC/ΔKJ cells, 112 PS proteins were further destabilized in NC/ΔKJ cells ($p = 0.004$), including 43 previously identified DnaK substrates (Calloni et al., 2012; Table S4D). The median fraction cleaved of these proteins shifted from 48% in NC cells to 81% in NC/ΔKJ cells (Figure 3C), which is consistent with KJ dependence for conformational maintenance. However, the overlap between the proteins stabilized by KJE upon HS (189) (Figure 2C) and the proteins that were destabilized in ΔKJ cells (112) (Figure 3C) is only 25 proteins. This suggests that constitutive deregulation of other chaperones in ΔKJ cells also contributes to protein destabilization.

Structural Properties of Protease-Sensitive Proteins

Next, we conducted bioinformatic analyses to understand how the sensitivity of proteins to PP correlates with their physicochemical and structural properties. As the reference set, the 1,306 proteins that were quantified under all growth conditions were used (Figure S5A). We found that thermo-sensitive (HS-TS) proteins—the set of 188 proteins that are significantly destabilized upon HS compared to NC (Table S2C)—are generally larger than average in size (Figure 4A), tend to have multiple domains (Figure S5B), and are more frequently found in hetero-oligomeric complexes (Figure S5C). Note that the shift to larger sizes is less pronounced for NC-PS proteins (Figure 4A). Thus, the enrichment of multi-domain proteins in the thermo-sensitive subproteome is not simply due to the presence of more potential cleavage sites in larger proteins, but does reflect a greater conformational instability. In contrast, the proteins that remain protease sensitive upon KJE overexpression or are destabilized (HS/KJE-TS proteins) are smaller than HS-TS proteins (Figure 4A). Most of these proteins (50%–70%) are single domain (Figure S5B) and tend to be monomeric, in contrast to the majority of soluble proteins (~58% of total), which are homo-oligomeric (Figure S5C). This observation also supports the notion that homo-oligomeric assembly confers conformational stability (Marsh and Teichmann, 2015). Conversely, proteins that are stabilized by KJE upon HS tend to be larger in size, less hydrophobic, and more frequently multi-domain or ribosomal than the control proteins (Figures 4A, 4B, S5B, and S5C).

The isoelectric point (pI) distribution of PS proteins is similar to that of the control set of all of the quantified proteins (Tables S2 and S3). PS and thermo-sensitive proteins are overall less hydrophobic than the control set (Figure 4B), which is

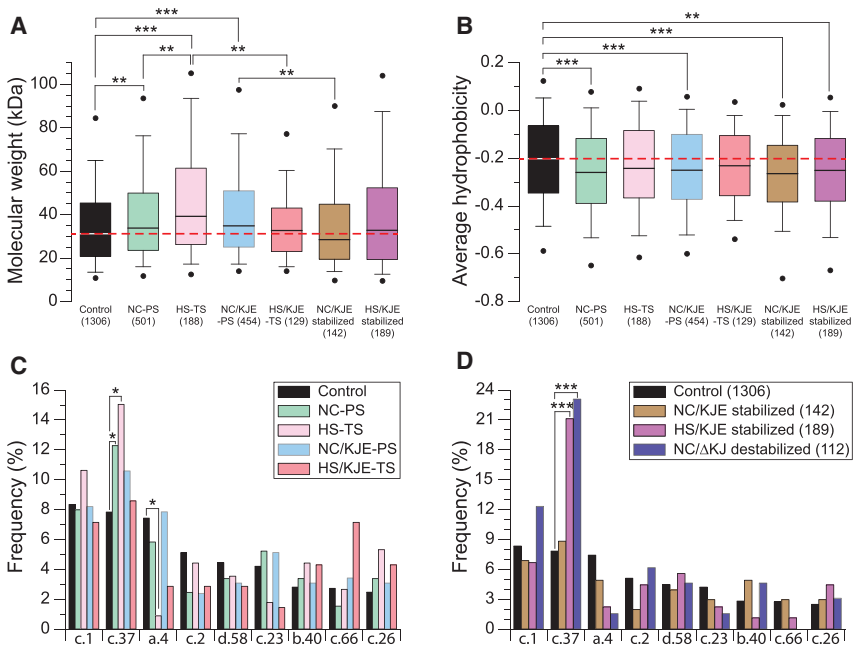

Figure 4. Structural Properties of Protease-Sensitive Proteins

(A and B) Molecular weight distribution (A) and average hydrophobicity (B) of NC-PS, HS-TS, NC/KJE-PS, HS/KJE-PS, NC/KJE stabilized, and HS/KJE stabilized proteins. The reference set comprises the 1,306 proteins quantified in all 4 conditions (Figure S5A). The horizontal lines in the boxplots indicate the median; whisker caps and circles indicate the 10th–90th and 5th–95th percentiles, respectively.

(C) SCOP fold domain distribution for the NC-PS, HS-TS, NC/KJE-PS, and HS/KJE-PS proteins. c.1, triosephosphate isomerase (TIM) β/α barrel; c.37, P loop containing nucleotide triphosphate hydrolases; a.4, DNA or RNA binding 3-helical bundle; c.2, NAD(P) (nicotinamide adenine dinucleotide phosphate)-binding Rossman-fold domains; d.58, ferredoxin-like; c.23, flavodoxin-like; b.40, oligonucleotide/oligosaccharide-binding (OB)-fold; c.66, S-adenosyl-L-methionine-dependent methyltransferases; c.26, adenine nucleotide α-hydrolase-like.

(D) SCOP fold distribution for the sets of proteins stabilized by KJE overexpression in NC (NC/KJE stabilized; 142 proteins) and HS (HS/KJE stabilized; 189 proteins) and for the proteins destabilized in ΔKJ cells (112 proteins).

The p value in (A) and (B) is based on the Mann-Whitney test, and the p value in (C) and (D) is based on a χ^2 test:;; *p ≤ 0.05, **p ≤ 0.01, and ***p ≤ 0.001.

consistent with findings that proteins with an extensive hydrophobic core are more stable and less aggregation prone (Walther et al., 2015).

To determine whether specific domain fold topologies are enriched in the PS proteome, we isolated the peptides generated by the thermolysin pulse through a filtration device and analyzed them by LC-MS/MS (see STAR Methods). We identified 1,824 thermolysin peptides at NC and 678 thermolysin peptides at HS, and assigned them to 369 NC-PS proteins and 125 HS-TS proteins, respectively (Tables S5A and S5B). The cleavage peptides of thermo-sensitive (HS-TS) proteins are more hydrophobic than those generated from NC-PS proteins or from chemically denatured lysate proteins (Figure S5D; Table S1A). This finding indicates that the unfolding induced by HS leads to the exposure of hydrophobic amino acids that are buried in the native state. We could assign 1,602 and 601 thermolysin cleavage peptides to known Structural Classification of Proteins (SCOP) fold domains for NC-PS and HS-TS proteins, respectively (Gough et al., 2001). We found that ~12% of NC-PS proteins (40 of 326 with known domain fold) and ~15% of HS-TS proteins (17 of 113 proteins) contained at least one PS domain with SCOP fold c.37 (P loop nucleotide triphosphate hydrolases), compared to ~8% in the control set (95 of 1,213 proteins) (Figure 4C). The domain fold c.37 is characterized by a complex α/β topology and is overrepresented (~18% of total) in the set of strong DnaK interactors identified previously (Calloni et al., 2012). Proteins with c.37 architecture are multifunctional and undergo conformational changes upon nucleotide binding and hydrolysis (Caetano-Anollés et al., 2009). The c.37 domain is often part of the multi-domain and hetero-oligomeric proteins (Calloni et al., 2012). c.37 domains in the context of multi-domain proteins are stabilized against thermal unfolding by KJE overexpression and are destabilized in ΔKJ cells (Figure 4D). In contrast, the SCOP fold a.4 (DNA or RNA binding 3-helical bundle) is underrepresented among TS proteins (Figure 4C), suggesting that this domain fold is generally rather thermo-stable. Note that the ribosomal proteins that are strongly stabilized by KJE (Figure S3E) belong to several SCOP folds, including b.40, b.34, d.58, and d.325. These proteins have a high degree of surface accessibility in the ribosome complex and represent a specific subset of thermo-sensitive proteins.

In summary, besides ribosomal proteins, the DnaK chaperone system conformationally stabilizes large multi-domain proteins with a preference for proteins containing c.37 domains. Proteins with such domains are frequently hetero-oligomeric. In contrast, the proteins that are destabilized by KJE are often monomeric, single-domain proteins.

The DnaK Chaperone System Stabilizes the Folded State of Thermo-sensitive Proteins

To understand at the structural level how the KJE system stabilizes proteins against stress-induced unfolding, we analyzed the PP-cleavage pattern of UvrA and FusA as examples of thermo-sensitive multi-domain proteins (Figure 2F). UvrA, a known DnaK interactor (Calloni et al., 2012), is part of a hetero-oligomeric complex in which a UvrA dimer interacts with two molecules of UvrB. UvrA has two discontinuous c.37 domains and contains multiple predicted DnaK binding sites throughout the sequence (Figure 5A). At 37°C (NC), UvrA is largely stable (Figure 2F). Only ~15% of molecules are cleaved upon PP at a single hydrophilic region at residues Thr703 and Glu713 (Figure 5A). Upon HS, the protein unfolds extensively (~50% of molecules cleaved), exposing at least 10 hydrophobic cleavage sites that

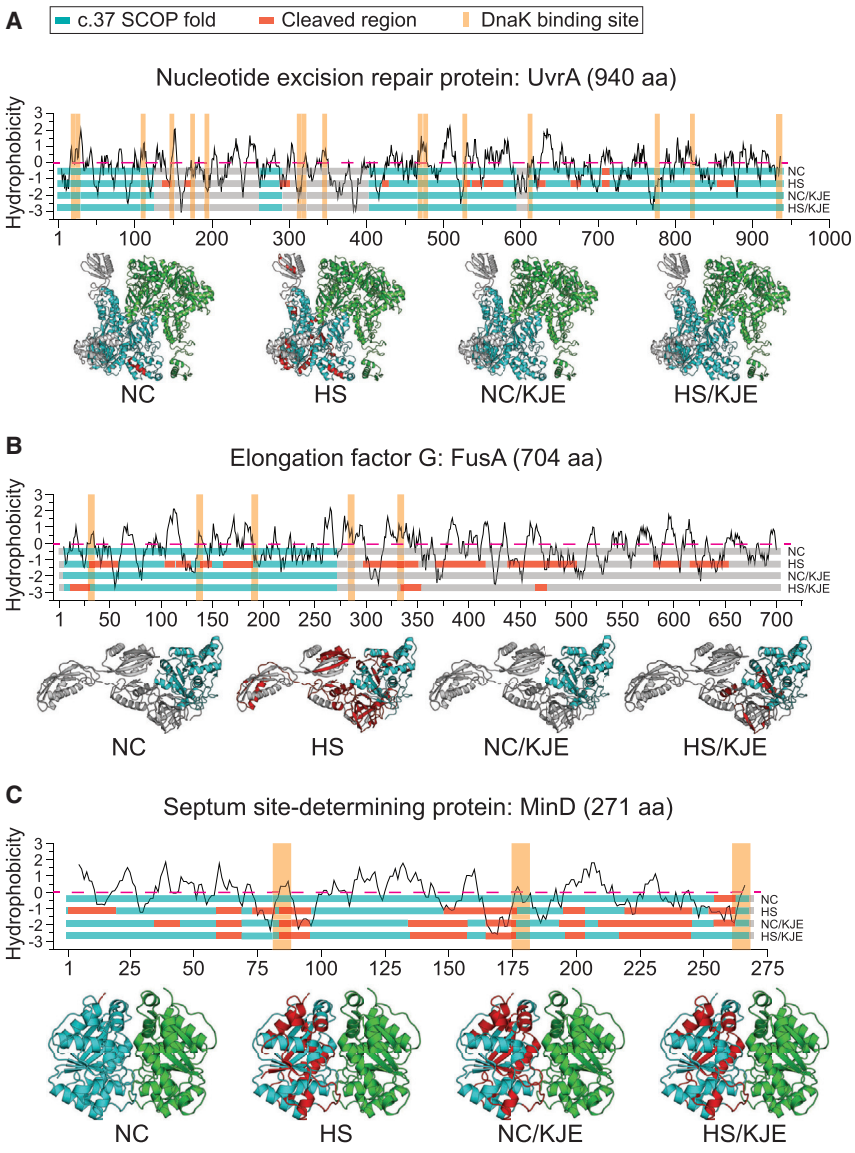

Figure 5. PP Analysis of Specific Thermosensitive Proteins

(A–C) Top: the PP-cleavage pattern of nucleotide excision repair protein UvrA (A), elongation factor G (FusA) (B), and septum site-determining protein MinD (C) are mapped to the amino acid sequences. The c.37 SCOP fold domains are in cyan and the other domains are in gray; the hydrophobicity profiles are shown. The predicted DnaK binding sites are indicated as vertical lines in orange. The regions of significant thermolysin cleavage are marked in red (see STAR Methods). Bottom: the cleaved regions (red) are assigned to the protein structures of UvrA (PDB: 2R6F, a homolog from *Bacillus stearothermophilus*), FusA (PDB: 3J0E), and MinD (PDB: 3Q9L). The protein domains are colored as at the top. In the case of UvrA and MinD, the cleavage pattern is displayed in only one subunit of the dimer; the opposite subunits are in green.

are inaccessible at 37°C (Figure 5A; Table S5B). Overexpression of KJE before HS efficiently protects UvrA against cleavage at all of these sites (Figure 5A) and fully restores its stability (~17% of molecules degraded) (Figure 2F). FusA (elongation factor G) is a 77-kDa protein consisting of 5 domains (SCOP folds c.37, b.34, d.58, d.14, and d.58), with most of the predicted DnaK binding sites located in the GTP-binding c.37 domain (Figure 5B). FusA is globally destabilized upon HS (60% cleaved) (Figure 2F), exposing 29 mostly hydrophobic thermolysin cleavage sites (Figure 5B). KJE overexpression is protective against cleavage at almost all of these sites.

The high degree of stabilization against PP afforded by KJE did not result from the prevention of protein aggregation, as only ~1.3% of UvrA and ~0.3% of FusA were recovered in the insoluble fraction upon HS (Table S2E). Thus, the KJE system either shifted the equilibrium of these proteins to the folded native state or shielded hydrophobic regions exposed upon thermal unfolding. To distinguish between these possibilities, we performed PP experiments *in vitro* using the thermo-labile model protein firefly luciferase (FLuc) (Schröder et al., 1993). FLuc denatured upon incubation at 45°C and formed a stable complex with DnaK/DnaJ in the presence of ATP and the absence of GrpE. Chaperone binding prevented FLuc aggregation but rendered the protein highly sensitive to PP with thermolysin at multiple cleavage sites (measured at 25°C) (Figure S6), ruling out a shielding effect. This observation indicates that ATP-dependent cycles of DnaK/DnaJ binding and release, mediated by GrpE, promote refolding even under otherwise denaturing conditions.

Next, we analyzed the PP-cleavage pattern of MinD, a homodimer of 29 kDa subunits, as an example of a protein that is destabilized by KJE (Figure 5C). MinD oscillates between cell poles and is deenriched in the midzone of the cell, thereby marking the midzone for cell division (Wu et al., 2011). It consists of a single c.37 domain. In NC cells, MinD is largely protease stable, except for cleavage of the short amphipathic α-helix at the C terminus (residues 255–263) that inserts transiently into the membrane during cycling (Wu et al., 2011; Figure 5C). Upon HS, cleavage occurred throughout the sequence, including the dimer interface, which is indicative of a shift to an unfolded monomer and is consistent with the temperature dependence of function (Touhami et al., 2006). Notably, KJE overexpression markedly destabilized MinD, even at NC, to an extent similar to HS (Figure 5C), suggesting that MinD is conformationally dynamic. Thus, the DnaK chaperone machinery can have opposing effects on protein stability, even for proteins with similar c.37 domain topologies.

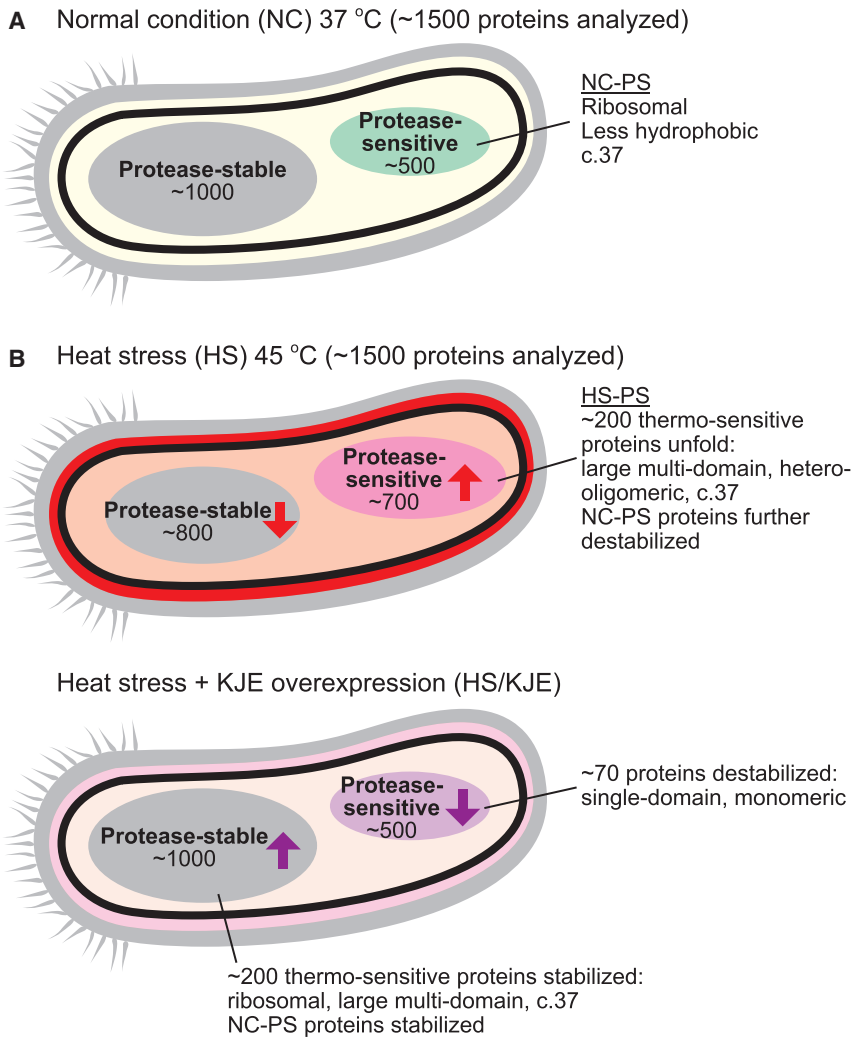

Figure 6. Effects of the DnaK Chaperone System on Proteome Stability

(A) Partitioning of the *E. coli* cytosolic proteome into protease-stable and PS (conformationally dynamic) proteins at the NC.

(B) Effect of acute HS on protein stability in the absence (top) and presence (bottom) of ~10×- elevated levels of the DnaK chaperone system. Numbers of protease-stable and PS proteins are indicated, as well as their characteristic physicochemical and structural properties. Arrow up indicates destabilization and arrow down indicates stabilization.

DISCUSSION

We have analyzed ~1,500 of the ~2,400 cytosolic proteins (Kerner et al., 2005) of *E. coli* by PP and quantitative proteomics and characterized the effects of the DnaK (Hsp70) chaperone system (KJE) on proteome stability. We found ~500 proteins (~25% of total by mass) to be protease sensitive (PS) under NCs, indicating that conformationally dynamic proteins make up a large fraction of the cytosolic proteome (Figure 6A). These metastable proteins tend to be larger than average in size, with a high degree of connectivity in protein interaction networks. Upon acute HS not resulting in the upregulation of the major chaperone systems, an additional ~200 proteins unfolded, exposing hydrophobic amino acid residues to the solvents that are buried in the native state. HS also resulted in a further destabilization of NC-PS proteins, increasing the fraction of cleaved proteins to ~33% by mass (Figure 6B). The overexpression of KJE revealed the potential of this chaperone system to markedly stabilize numerous thermo-sensitive proteins, including ribosomal proteins and large, multi-domain, hetero-oligomeric proteins (Figure 6B). These results reveal a previously unknown capacity of Hsp70 to stabilize proteins in their folded states under denaturing stress conditions.

Properties of Thermo-sensitive Proteins Stabilized by KJE

The DnaK chaperone system had a profound effect on proteome stability by restoring the folding equilibrium of many thermo-sensitive proteins to a level comparable to that observable at normal temperature (Figure 6B). A large fraction of these stabilized proteins have previously been identified as DnaK interactors (Calloni et al., 2012), as exemplified by UvrA and FusA. These KJE-stabilized proteins frequently contain c.37 domains, which are significantly enriched among thermo-sensitive proteins, and are typically multi-domain and part of the hetero-oligomeric complexes. c.37 is evolutionarily the most ancient and also one of the most abundant protein folds in *E. coli*, comprising many essential nucleotide-binding enzymes that are often part of the hetero-oligomeric complexes (Ma et al., 2008; McGuffin et al., 2004). The c.37 α/β topology is stabilized by extensive long-range interactions. Accordingly, such proteins tend to have complex folding pathways and are likely to populate kinetically trapped folding intermediates (Gromiha and Selvaraj, 2004), during both folding and unfolding. These findings suggest that thermo-labile protein domains have co-evolved with the DnaK chaperone system to optimize (functionally relevant) structural dynamics, while avoiding global destabilization and loss of function under stress conditions.

Stabilization by KJE is also prominent for numerous essential ribosomal proteins, assigning an important ribosome-protective role to this chaperone system at an elevated temperature. Ribosomal proteins are overall highly positively charged, and it is tempting to speculate that the binding specificity of DnaK for short hydrophobic sequence elements that are flanked by basic amino acids (Rüdiger et al., 1997) represents an adaptation to this highly conserved protein class. Such an adaptation could then have shaped the general mode of interaction of DnaK with client proteins.

Mechanistic Considerations

How does the DnaK system conformationally stabilize proteins under denaturing HS conditions? We demonstrated that the binding of DnaK to a thermally denatured model protein *in vitro* resulted in global destabilization and extensive cleavage upon PP, excluding a mechanism of protease protection by direct shielding of hydrophobic cleavage sites. We therefore conclude that the DnaK chaperone system actively promotes refolding or prevents unfolding, even under conditions in which the native state is thermodynamically unfavorable. The mechanism underlying this remarkable capacity remains to be explored, but our results are consistent with recent observations *in vitro* (Goloubinoff et al., 2018; Mashaghi et al., 2016), including the proposal that DnaK may not only bind unfolded proteins but also transiently interact with and stabilize near-native states (Mashaghi et al., 2016). DnaK may also destabilize kinetically trapped (un)folding intermediates populated upon HS, thereby facilitating refolding and shifting the folding equilibrium toward the native state. Support for the notion that kinetically trapped folding intermediates accumulate upon HS comes from the fact that thermo-sensitive proteins do not readily refold upon the transfer of cells from 45°C to 37°C, the temperature of PP. We note that this putative mechanism of Hsp70 action provides both a target (i.e., exposed hydrophobic residues in the intermediate that are normally buried in the folded state) and efficiency, as intermediate states are much less populated than native states, and therefore there is a much lower chaperone requirement.

Destabilizing Effects of KJE

Our analysis revealed that elevated KJE levels, while being largely proteome protective, have a trade-off in destabilizing a minor group of proteins (Figure 6B). These proteins are generally smaller in size and often monomeric, and DnaK binding apparently shifts their folding equilibrium toward the unfolded state. We suggest that this mechanism may contribute to the adaptation of *E. coli* to stress conditions. A prominent example of this type of protein is heat shock regulator rpoH (σ^{32}) (~31 kDa), in which destabilization by high levels of DnaK serves to attenuate the stress response (Rodriguez et al., 2008). Another example is the cell division protein MinD, a thermo-labile protein that is markedly destabilized by elevated KJE levels, even at NC. The inhibition of MinD function causes minicell formation, which was proposed to facilitate the disposal of damaged proteins under stress conditions (de Boer et al., 1989; Rang et al., 2018), suggesting that destabilization by KJE may be physiologically relevant. As MinD consists of a single c.37 domain, these findings show that the chaperone machinery can have opposing effects on protein stability, even for proteins with similar c.37 domain topologies. Whether the chaperones shift the folding equilibrium toward the native state (UvrA, FusA) or are destabilizing (MinD) appears to depend on a complex interplay of factors, including intrinsic structural stability and folding properties, domain context (multi- or single-domain proteins), and the number and location of potential DnaK binding regions.

Overall, these findings reveal how the levels of DnaK (and of molecular chaperones in general) must be carefully controlled and adjusted to growth conditions to achieve the optimal balance between the opposing effects on protein stability.

STAR★METHODS

Detailed methods are provided in the online version of this paper and include the following:

- KEY RESOURCES TABLE
- LEAD CONTACT AND MATERIALS AVAILABILITY
- EXPERIMENTAL MODEL AND SUBJECT DETAILS
- METHOD DETAILS
  - SILAC Medium
  - Protein Purification
  - Cell Culture
  - Cell Lysis and Pulse Proteolysis
  - Sucrose Density Gradient
  - Isolation of Protein Aggregates Under Normal Growth and Heat Stress Conditions
  - Analysis of Thermolysin Cleaved Peptides
  - SDS-PAGE and In-gel Digestion with Trypsin
  - Sample Preparation for Analysis of Total Proteome and Protein Aggregates
  - Mass Spectrometry
  - Database Search
  - Cutoff Control Experiment
  - Data Processing
- QUANTIFICATION AND STATISTICAL ANALYSIS
  - Bioinformatic Analysis
- DATA AND CODE AVAILABILITY

SUPPLEMENTAL INFORMATION

Supplemental Information can be found online at https://doi.org/10.1016/j.celrep.2019.06.081.

ACKNOWLEDGMENTS

The technical assistance by Albert Ries is gratefully acknowledged. We thank Beatrice Ramm, Andreas Bracher, Chandhuru Jagadeesan, and Rahmi Imamoglu for fruitful discussions. This work was funded in part by the Minerva Foundation, the Munich Center for Integrated Protein Science (CIPSM), and the Deutsche Forschungsgemeinschaft (SFB 1035). The work by G.V. and M.V. was supported by the Centre for Misfolding Diseases, Department of Chemistry, University of Cambridge.

AUTHOR CONTRIBUTIONS

L.Z., R.K., M.H.-H., and F.U.H. conceived the study and designed the experiments. L.Z. performed the biochemical and proteomics experiments and carried out the data analysis with help from R.K. L.Z., G.V., and M.V. performed the bioinformatic analyses. L.Z., R.K., M.H.-H., and F.U.H. wrote the manuscript with input from all of the authors.

DECLARATION OF INTERESTS

The authors declare no competing interests.

Received: March 11, 2019
Revised: June 1, 2019
Accepted: June 21, 2019
Published: July 30, 2019

REFERENCES

Adhikari, J., and Fitzgerald, M.C. (2014). SILAC-pulse proteolysis: a mass spectrometry-based method for discovery and cross-validation in proteome-wide studies of ligand binding. J. Am. Soc. Mass Spectrom. *25*, 2073–2083.

Arsène, F., Tomoyasu, T., and Bukau, B. (2000). The heat shock response of Escherichia coli. Int. J. Food Microbiol. *55*, 3–9.

Balch, W.E., Morimoto, R.I., Dillin, A., and Kelly, J.W. (2008). Adapting proteostasis for disease intervention. Science *319*, 916–919.

Balchin, D., Hayer-Hartl, M., and Hartl, F.U. (2016). In vivo aspects of protein folding and quality control. Science *353*, aac4354.

Bardwell, J.C., and Jakob, U. (2012). Conditional disorder in chaperone action. Trends Biochem. Sci. *37*, 517–525.

Bhandari, V., and Houry, W.A. (2015). Substrate Interaction Networks of the Escherichia coli Chaperones: Trigger Factor, DnaK and GroEL. Adv. Exp. Med. Biol. *883*, 271–294.

Buchberger, A., Theyssen, H., Schröder, H., McCarty, J.S., Virgallita, G., Milkereit, P., Reinstein, J., and Bukau, B. (1995). Nucleotide-induced conformational changes in the ATPase and substrate binding domains of the DnaK chaperone provide evidence for interdomain communication. J. Biol. Chem. *270*, 16903–16910.

Bukau, B., and Walker, G.C. (1989). Cellular defects caused by deletion of the Escherichia coli dnaK gene indicate roles for heat shock protein in normal metabolism. J. Bacteriol. *171*, 2337–2346.

Caetano-Anollés, G., Wang, M., Caetano-Anollés, D., and Mittenthal, J.E. (2009). The origin, evolution and structure of the protein world. Biochem. J. *417*, 621–637.

Calloni, G., Chen, T., Schermann, S.M., Chang, H.C., Genevaux, P., Agostini, F., Tartaglia, G.G., Hayer-Hartl, M., and Hartl, F.U. (2012). DnaK functions as a central hub in the E. coli chaperone network. Cell Rep. *1*, 251–264.

Castanié, M.P., Bergès, H., Oreglia, J., Prère, M.F., and Fayet, O. (1997). A set of pBR322-compatible plasmids allowing the testing of chaperone-assisted folding of proteins overexpressed in Escherichia coli. Anal. Biochem. *254*, 150–152.

Chen, K., Gao, Y., Mih, N., O'Brien, E.J., Yang, L., and Palsson, B.O. (2017). Thermosensitivity of growth is determined by chaperone-mediated proteome reallocation. Proc. Natl. Acad. Sci. USA *114*, 11548–11553.

Clerico, E.M., Tilitsky, J.M., Meng, W., and Gierasch, L.M. (2015). How hsp70 molecular machines interact with their substrates to mediate diverse physiological functions. J. Mol. Biol. *427*, 1575–1588.

Cox, J., and Mann, M. (2008). MaxQuant enables high peptide identification rates, individualized p.p.b.-range mass accuracies and proteome-wide protein quantification. Nat. Biotechnol. *26*, 1367–1372.

de Boer, P.A., Crossley, R.E., and Rothfield, L.I. (1989). A division inhibitor and a topological specificity factor coded for by the minicell locus determine proper placement of the division septum in E. coli. Cell *56*, 641–649.

Deuerling, E., Schulze-Specking, A., Tomoyasu, T., Mogk, A., and Bukau, B. (1999). Trigger factor and DnaK cooperate in folding of newly synthesized proteins. Nature *400*, 693–696.

Feng, Y., De Franceschi, G., Kahraman, A., Soste, M., Melnik, A., Boersema, P.J., de Laureto, P.P., Nikolaev, Y., Oliveira, A.P., and Picotti, P. (2014). Global analysis of protein structural changes in complex proteomes. Nat. Biotechnol. *32*, 1036–1044.

Frydman, J. (2001). Folding of newly translated proteins in vivo: the role of molecular chaperones. Annu. Rev. Biochem. *70*, 603–647.

Genevaux, P., Keppel, F., Schwager, F., Langendijk-Genevaux, P.S., Hartl, F.U., and Georgopoulos, C. (2004). In vivo analysis of the overlapping functions of DnaK and trigger factor. EMBO Rep. *5*, 195–200.

Gershenson, A., Gierasch, L.M., Pastore, A., and Radford, S.E. (2014). Energy landscapes of functional proteins are inherently risky. Nat. Chem. Biol. *10*, 884–891.

Goloubinoff, P., Sassi, A.S., Fauvet, B., Barducci, A., and De Los Rios, P. (2018). Chaperones convert the energy from ATP into the nonequilibrium stabilization of native proteins. Nat. Chem. Biol. *14*, 388–395.

Gough, J., Karplus, K., Hughey, R., and Chothia, C. (2001). Assignment of homology to genome sequences using a library of hidden Markov models that represent all proteins of known structure. J. Mol. Biol. *313*, 903–919.

Gromiha, M.M., and Selvaraj, S. (2004). Inter-residue interactions in protein folding and stability. Prog. Biophys. Mol. Biol. *86*, 235–277.

Hoyer, W., Antony, T., Cherny, D., Heim, G., Jovin, T.M., and Subramaniam, V. (2002). Dependence of alpha-synuclein aggregate morphology on solution conditions. J. Mol. Biol. *322*, 383–393.

Huang, W., Sherman, B.T., and Lempicki, R.A. (2009). Systematic and integrative analysis of large gene lists using DAVID bioinformatics resources. Nat. Protoc. *4*, 44–57.

Kerner, M.J., Naylor, D.J., Ishihama, Y., Maier, T., Chang, H.C., Stines, A.P., Georgopoulos, C., Frishman, D., Hayer-Hartl, M., Mann, M., and Hartl, F.U. (2005). Proteome-wide analysis of chaperonin-dependent protein folding in Escherichia coli. Cell *122*, 209–220.

Lakshmipathy, S.K., Gupta, R., Pinkert, S., Etchells, S.A., and Hartl, F.U. (2010). Versatility of trigger factor interactions with ribosome-nascent chain complexes. J. Biol. Chem. *285*, 27911–27923.

Langer, T., Lu, C., Echols, H., Flanagan, J., Hayer, M.K., and Hartl, F.U. (1992). Successive action of DnaK, DnaJ and GroEL along the pathway of chaperone-mediated protein folding. Nature *356*, 683–689.

Leuenberger, P., Ganscha, S., Kahraman, A., Cappelletti, V., Boersema, P.J., von Mering, C., Claassen, M., and Picotti, P. (2017). Cell-wide analysis of protein thermal unfolding reveals determinants of thermostability. Science *355*, eaai7825.

Ma, B.G., Chen, L., Ji, H.F., Chen, Z.H., Yang, F.R., Wang, L., Qu, G., Jiang, Y.Y., Ji, C., and Zhang, H.Y. (2008). Characters of very ancient proteins. Biochem. Biophys. Res. Commun. *366*, 607–611.

Marsh, J.A., and Teichmann, S.A. (2015). Structure, dynamics, assembly, and evolution of protein complexes. Annu. Rev. Biochem. *84*, 551–575.

Mashaghi, A., Bezrukavnikov, S., Minde, D.P., Wentink, A.S., Kityk, R., Zachmann-Brand, B., Mayer, M.P., Kramer, G., Bukau, B., and Tans, S.J. (2016). Alternative modes of client binding enable functional plasticity of Hsp70. Nature *539*, 448–451.

Mayer, M.P. (2013). Hsp70 chaperone dynamics and molecular mechanism. Trends Biochem. Sci. *38*, 507–514.

Mayer, M.P., and Bukau, B. (2005). Hsp70 chaperones: cellular functions and molecular mechanism. Cell. Mol. Life Sci. *62*, 670–684.

Mayer, M.P., and Gierasch, L.M. (2019). Recent advances in the structural and mechanistic aspects of Hsp70 molecular chaperones. J. Biol. Chem. *294*, 2085–2097.

McGuffin, L.J., Street, S.A., Bryson, K., Sørensen, S.A., and Jones, D.T. (2004). The Genomic Threading Database: a comprehensive resource for structural annotations of the genomes from key organisms. Nucleic Acids Res. *32*, D196–D199.

Mogk, A., Tomoyasu, T., Goloubinoff, P., Rüdiger, S., Röder, D., Langen, H., and Bukau, B. (1999). Identification of thermolabile Escherichia coli proteins: prevention and reversion of aggregation by DnaK and ClpB. EMBO J. *18*, 6934–6949.

Park, C., and Marqusee, S. (2005). Pulse proteolysis: a simple method for quantitative determination of protein stability and ligand binding. Nat. Methods *2*, 207–212.

Park, C., Zhou, S., Gilmore, J., and Marqusee, S. (2007). Energetics-based protein profiling on a proteomic scale: identification of proteins resistant to proteolysis. J. Mol. Biol. *368*, 1426–1437.

Rang, C.U., Proenca, A., Buetz, C., Shi, C., and Chao, L. (2018). Minicells as a damage disposal mechanism in Escherichia coli. MSphere *3*, e00428-e18.

Rappsilber, J., Mann, M., and Ishihama, Y. (2007). Protocol for micro-purification, enrichment, pre-fractionation and storage of peptides for proteomics using StageTips. Nat. Protoc. *2*, 1896–1906.

René, O., and Alix, J.H. (2011). Late steps of ribosome assembly in E. coli are sensitive to a severe heat stress but are assisted by the HSP70 chaperone machine. Nucleic Acids Res. *39*, 1855–1867.

Rodriguez, F., Arsène-Ploetze, F., Rist, W., Rüdiger, S., Schneider-Mergener, J., Mayer, M.P., and Bukau, B. (2008). Molecular basis for regulation of the heat shock transcription factor sigma32 by the DnaK and DnaJ chaperones. Mol. Cell *32*, 347–358.

Rüdiger, S., Germeroth, L., Schneider-Mergener, J., and Bukau, B. (1997). Substrate specificity of the DnaK chaperone determined by screening cellulose-bound peptide libraries. EMBO J. *16*, 1501–1507.

Schmidt, A., Kochanowski, K., Vedelaar, S., Ahrné, E., Volkmer, B., Callipo, L., Knoops, K., Bauer, M., Aebersold, R., and Heinemann, M. (2016). The quantitative and condition-dependent Escherichia coli proteome. Nat. Biotechnol. *34*, 104–110.

Schröder, H., Langer, T., Hartl, F.U., and Bukau, B. (1993). DnaK, DnaJ and GrpE form a cellular chaperone machinery capable of repairing heat-induced protein damage. EMBO J. *12*, 4137–4144.

Tang, Y.C., Chang, H.C., Roeben, A., Wischnewski, D., Wischnewski, N., Kerner, M.J., Hartl, F.U., and Hayer-Hartl, M. (2006). Structural features of the GroEL-GroES nano-cage required for rapid folding of encapsulated protein. Cell *125*, 903–914.

Tatusov, R.L., Galperin, M.Y., Natale, D.A., and Koonin, E.V. (2000). The COG database: a tool for genome-scale analysis of protein functions and evolution. Nucleic Acids Res. *28*, 33–36.

Teter, S.A., Houry, W.A., Ang, D., Tradler, T., Rockabrand, D., Fischer, G., Blum, P., Georgopoulos, C., and Hartl, F.U. (1999). Polypeptide flux through bacterial Hsp70: DnaK cooperates with trigger factor in chaperoning nascent chains. Cell *97*, 755–765.

Tomoyasu, T., Mogk, A., Langen, H., Goloubinoff, P., and Bukau, B. (2001). Genetic dissection of the roles of chaperones and proteases in protein folding and degradation in the Escherichia coli cytosol. Mol. Microbiol. *40*, 397–413.

Tompa, P., and Kovacs, D. (2010). Intrinsically disordered chaperones in plants and animals. Biochem. Cell Biol. *88*, 167–174.

Touhami, A., Jericho, M., and Rutenberg, A.D. (2006). Temperature dependence of MinD oscillation in Escherichia coli: running hot and fast. J. Bacteriol. *188*, 7661–7667.

Tran, D.T., Adhikari, J., and Fitzgerald, M.C. (2014). StableIsotope Labeling with Amino Acids in Cell Culture (SILAC)-based strategy for proteome-wide thermodynamic analysis of protein-ligand binding interactions. Mol. Cell. Proteomics *13*, 1800–1813.

Tyanova, S., Temu, T., Sinitcyn, P., Carlson, A., Hein, M.Y., Geiger, T., Mann, M., and Cox, J. (2016). The perseus computational platform for comprehensive analysis of (prote)omics data. Nat. Methods *13*, 731–740.

Van Durme, J., Maurer-Stroh, S., Gallardo, R., Wilkinson, H., Rousseau, F., and Schymkowitz, J. (2009). Accurate prediction of DnaK-peptide binding via homology modelling and experimental data. PLoS Comput. Biol. *5*, e1000475.

Walther, D.M., Kasturi, P., Zheng, M., Pinkert, S., Vecchi, G., Ciryam, P., Morimoto, R.I., Dobson, C.M., Vendruscolo, M., Mann, M., and Hartl, F.U. (2015). Widespread proteome remodeling and aggregation in aging C. elegans. Cell *161*, 919–932.

Winkler, J., Seybert, A., König, L., Pruggnaller, S., Haselmann, U., Sourjik, V., Weiss, M., Frangakis, A.S., Mogk, A., and Bukau, B. (2010). Quantitative and spatio-temporal features of protein aggregation in Escherichia coli and consequences on protein quality control and cellular ageing. EMBO J. *29*, 910–923.

Wiśniewski, J.R., Zougman, A., and Mann, M. (2009). Combination of FASP and StageTip-based fractionation allows in-depth analysis of the hippocampal membrane proteome. J. Proteome Res. *8*, 5674–5678.

Wolff, S., Weissman, J.S., and Dillin, A. (2014). Differential scales of protein quality control. Cell *157*, 52–64.

Wu, S., and Zhu, Y. (2012). ProPAS: standalone software to analyze protein properties. Bioinformation *8*, 167–169.

Wu, W., Park, K.T., Holyoak, T., and Lutkenhaus, J. (2011). Determination of the structure of the MinD-ATP complex reveals the orientation of MinD on the membrane and the relative location of the binding sites for MinE and MinC. Mol. Microbiol. *79*, 1515–1528.

Wuchty, S., and Uetz, P. (2014). Protein-protein interaction networks of E. coli and S. cerevisiae are similar. Sci. Rep. *4*, 7187.

Yu, N.Y., Laird, M.R., Spencer, C., and Brinkman, F.S. (2011). PSORTdb–an expanded, auto-updated, user-friendly protein subcellular localization database for Bacteria and Archaea. Nucleic Acids Res. *39*, D241–D244.

STAR★METHODS

KEY RESOURCES TABLE

REAGENT or RESOURCE	SOURCE	IDENTIFIER
Bacterial and Virus Strains		
E. coli MC4100	(Genevaux et al., 2004)	N/A
E. coli MC4100 ΔdnaKdnaJ::Kan^R	(Genevaux et al., 2004)	N/A
E. coli MC4100 dnaKdnaJ-grpE::Kan^R Spc^R overexpression	(Castanié et al., 1997)	N/A
E. coli BL21 (DE3)	Agilent Technologies	Cat#200131
E. coli DH5α	ThermoFisher	Cat#18265017
Chemicals, Peptides, and Recombinant Proteins		
Mouse α-synuclein	(Hoyer et al., 2002)	N/A
Maltose-binding protein	(Tang et al., 2006)	N/A
DnaK	(Langer et al., 1992)	N/A
DnaJ	(Langer et al., 1992)	N/A
Lysozyme	Sigma	Cat#L6876
QuantiLum Recombinant Luciferase	Promega	Cat#E1701
L-Lysine light	Sigma	Cat#L8662
L-Arginine light	Sigma	Cat#11039
SILAC middle L-Lysine (4.4′.5.5′-D4-L-Lysine 2HCl)	Silantes	Cat#211104113
SILAC middle L-Arginine ($^{13}C_6$-L-Arginine HCl)	Cambridge Isotope Laboratories	Cat#CLM-2265-H
SILAC heavy L-Lysine ($^{13}C_6$ $^{15}N_2$-L-Lysine HCl)	Silantes	Cat#211604102
SILAC heavy L-Arginine ($^{13}C_6$ $^{15}N_4$-L-Arginine HCl)	Silantes	Cat#201604102
Thermolysin	Sigma	Cat#T7902
EDTA-free protease inhibitor	Sigma (Roche)	Cat#04693159001
Trypsin recombinant, Proteomics Grade	Sigma (Roche)	Cat#03708969001
Empore SPE Disks C18, Diam. 47 mm, pk of 20	Sigma	Cat#66883-U
Empore SPE Disks Cation Exchange-SR, Diam. 47 mm, pk of 20	Sigma	Cat#66889-U
Amicon Ultra-0.5 mL Centrifugal Filters	EMD Millipore	Cat#UFC501096
Critical Commercial Assays		
BCA protein assay	Pierce	Cat#23228
Data and Code Availability		
Proteomic data	This paper	PRIDE: PXD012929 (https://www.ebi.ac.uk/pride/archive/)
Plasmid		
pOFX tac-JKE1	(Castanié et al., 1997)	N/A
pSTS500 α-synuclein	(Lakshmipathy et al., 2010)	N/A
D95C MBP	(Tang et al., 2006)	N/A
pET11d DnaK	(Langer et al., 1992)	N/A
pET11a DnaJ	(Langer et al., 1992)	N/A
Software and Algorithms		
Perseus v.1.5.0.9	(Tyanova et al., 2016)	https://www.ncbi.nlm.nih.gov/pubmed/?term=Nat+Methods+2016+Perseus
MaxQuant 1.5.0.25	(Cox and Mann, 2008)	https://www.maxquant.org/
RStudio	RStudio	https://www.rstudio.com
R version v. 3.3.1	The R foundation	https://www.r-project.org/
PyMOL 1.7	DeLano Scientific	PRID: SCR_000305

(*Continued on next page*)

Continued

REAGENT or RESOURCE	SOURCE	IDENTIFIER
SigmaPlot 12.0	Systat Software, Inc.	N/A
OriginPro 9.1	OriginLab	PRID: SCR_015636
SCOP 1.73 classification	(Gough et al., 2001)	http://supfam.org/SUPERFAMILY/downloads.html
pSORT 3.0	(Yu et al., 2011)	https://www.psort.org/psortb/
ProPAS	(Wu and Zhu, 2012)	http://bioinfo.hupo.org.cn/tools/ProPAS/propas.htm
Limbo	(Van Durme et al., 2009)	http://limbo.switchlab.org
Other		
ExPASy	Bioinformatic Resource Portal	https://web.expasy.org/protscale/
Clusters of Orthologous Groups of proteins (COG) database	(Tatusov et al., 2000)	https://www.ncbi.nlm.nih.gov/COG/

LEAD CONTACT AND MATERIALS AVAILABILITY

Further information and requests for resources and reagents should be directed to the Lead Contact, F. Ulrich Hartl (uhartl@biochem.mpg.de).

EXPERIMENTAL MODEL AND SUBJECT DETAILS

Experiments were carried out in *E. coli* strains MC4100, MC4100 Δ*dnaKdnaJ*::Kan^R (ΔKJ) (Genevaux et al., 2004) and MC4100 *dnaK-dnaJ-grpE*::Kan^{R}Spc^R (KJE overexpression) (Castanié et al., 1997).

METHOD DETAILS

SILAC Medium

M63 minimal medium supplemented with 0.2% glucose, 0.5 mM L-amino acid, and 1 mM $MgSO_4$ was used for SILAC labeling. To prepare light, medium and heavy media, the respective amino acids were added, for light: Arg0 and Lys0 (arginine and lysine, Sigma), for medium: Arg6 and Lys4 (13C6-L-arginine, Cambridge Isotope laboratories; 4.4′.5.5′-D4-L-lysine, Silantes) and for heavy: Arg10 and Lys8 (argine-$^{13}C_6$, $^{15}N_4$ and lysine-$^{13}C_6$, $^{15}N_2$, Silantes).

Protein Purification

Mouse α-synuclein (α-Syn) (pSTS500 plasmid, WT), maltose binding protein MBP (ECB/pBA), DnaK and DnaJ were expressed in *E. coli* cells (strain BL21, DE3). For the purification of α-Syn and MBP, cells were grown in light and heavy isotope labeled medium at 37°C, respectively, while for purification of DnaK and DnaJ, cells were grown in LB medium. Induction was carried out at an OD_{600nm} of ∼0.5 with 1 mM isopropyl-β-D-thiogalactopyranoside (IPTG) for 2 h. The purification of these recombinant proteins was performed as described previously (Hoyer et al., 2002; Langer et al., 1992; Tang et al., 2006). The identity and purity of the isolated proteins was determined by LC-MS/MS. α-Syn and MBP were ∼98% pure based on intensity based absolute quantification (iBAQ). Purified proteins were stored in 10 mM HEPES buffer (pH 7.4) containing 5% (v/v) glycerol at −80°C.

Cell Culture

E. coli cells (WT and Δ*dnaKdnaJ*::Kan^R strain) were grown to an OD_{600nm} of ∼1 under normal growth (NC) conditions at 37°C in 25 mL light (L) or heavy (H) SILAC medium. For expression of the *dnaK-dnaJ-grpE* chaperone machinery, induction was carried out with 250 μM IPTG when cells reached mid-exponential phase (OD_{600nm} ∼0.5). To isolate the insoluble fraction, *E. coli* cells were grown in 25 mL light (L), medium (M) or heavy (H) SILAC medium at 37°C. Cells were harvested at OD_{600nm} ∼1. Spheroplasts were prepared at 4°C as described previously (Calloni et al., 2012), then resuspended in 150 μL SILAC medium supplemented with 0.25 M sucrose, 0.2% glycerol and recovered at physiological temperature (37°C) for 15 min. For pulse proteolysis (PP) under heat stress, spheroplasts were incubated at 45°C for 15 min. Immediately after incubation at 37°C or 45°C, H-labeled purified proteins (3.9 μg α-Syn and 4.2 μg MBP) were added into the suspension of H-labeled cells as a control for PP efficiency.

Cell Lysis and Pulse Proteolysis

Spheroplasts (H-labeled) prepared as above were lysed by dilution into 350 μL hypo-osmotic lysis buffer (20 mM HEPES pH 7.4, 5 mM $CaCl_2$ and 5 mM $MgCl_2$) in the presence of ∼120 μg/mL thermolysin. To perform PP uniformly at 37°C, the temperature of the lysis buffer was 37°C for the normal growth condition (NC) and 34°C for the HS condition. Thermolysin treatment was terminated after 1 min by

addition of 100 μL stop-solution (6x protease inhibitor and 150 mM EDTA). The L-labeled purified proteins (α-Syn and MBP) were added into the H-labeled cell lysate in an amount equivalent to that of the H-labeled purified proteins (added before PP) as control for PP efficiency. L-labeled cells were lysed under the same conditions but without thermolysin treatment and addition of purified proteins. After centrifugation at 16 000 g for 15 min, 15 μg of light and heavy isotope labeled soluble cell lysates (from normal and heat stress conditions) were mixed 1:1. All experiments were conducted three times independently.

For PP on firefly luciferase (FLuc) bound to DanK/DnaJ, purified FLuc (0.1 μM) was incubated in the presence of DnaK (3 μM) and DnaJ (1 μM) at 25°C or 45°C for 30 min in HEPES buffer (25 mM HEPES, pH 7.5, 100 mM KCl, 5mM ATP, 10 mM $Mg(OAc)_2$). Then, proteins were subjected to PP (1 min at 25°C). After the reaction was stopped by the addition of EDTA (final concentration 25 mM), the samples were processed as described for the PP workflow. Three independent experiments were performed.

To perform PP of purified DnaK, trypsin or thermolysin (~120 μg/mL) was added to 3 μM DnaK in HEPES buffer (25 mM HEPES, pH 7.5, 100 mM KCl, 5mM ATP, 10 mM $Mg(OAc)_2$,) at 37°C. After 1 min incubation, the reaction was blocked by adding PMSF (final concentration 5 mM) for trypsin or EDTA (25 mM) for thermolysin. Samples were analyzed by SDS-PAGE on 4%–12% Bis-Tris acrylamide NuPAGE gels in MOPS SDS running buffer (Invitrogen) and stained with Coomassie Brilliant Blue.

To measure changes in the total proteome composition upon heat stress (HS cells H-labeled versus NC cells L-labeled), upon DnaK/DnaJ/GrpE overexpression (KJE cells L-labeled versus control cells H-labeled) or upon DnaK/DnaJ deletion (ΔKJ cells H-labeled versus NC cells L-labeled), spheroplasts were prepared as above and lysed in hypo-osmotic buffer (20 mM HEPES pH 7.4, 5 mM $CaCl_2$, 5 mM $MgCl_2$, 0.1% Triton and 6xEDTA free protease inhibitor). After centrifugation at 2,000 g for 15 min, 50 μg of L- and H-labeled cell lysates were mixed 1:1. All experiments were conducted three times independently.

To measure changes in the total proteome composition upon prolonged heat stress, L-labeled intact cells were incubated at 45°C for 3 h while control cells (H-labeled) were grown at 37°C. These cells were lysed by sonication. After centrifugation at 2,000 g for 15 min, 50 μg of L- and H-labeled cell lysates were mixed 1:1. Experiments were conducted two times independently.

Sucrose Density Gradient

Spheroplasts were prepared from WT cells grown at 37°C, as described above, and incubated at 15 min at 37°C (NC) or 15 min at 45°C (HS). Spheroplasts were lysed in hypo-osmotic lysis buffer (50 mM Tris (pH 7.4), 100 mM NaCl, 5 mM $MgCl_2$, 0.5% triton, 1x complete protease inhibitor EDTA-free, 1 mM PMSF and 1 mM chloramphenicol). RNA concentrations were determined using a NanoDrop UV spectrophotometer (Thermo Fisher). Equivalent amounts of RNA were layered onto a linear sucrose gradient (10 to 40% sucrose (w/v), 50 mM Tris (pH 7.4), 100 mM NaCl, 5 mM $MgCl_2$, and 1 mM chloramphenicol in nuclease-free water) and centrifuged in a SW41 rotor for 2 h at 36,000 rpm at 4°C. The gradient profile (absorbance at 254 nm) was analyzed using a piston gradient fractionator coupled to a spectrophotometer (BioComp).

Isolation of Protein Aggregates Under Normal Growth and Heat Stress Conditions

To isolate insoluble proteins, the spheroplasts prepared above were resuspended in 150 μL SILAC medium supplemented with 0.25 M sucrose, 0.2% glycerol and recovered at physiological temperature (37°C) for 15 min. The L- and H-labeled cells were further incubated at 45°C for 15 min. Cells were then lysed in hypo-osmotic buffer (20 mM HEPES pH 7.4, 5 mM $CaCl_2$, 5 mM $MgCl_2$, 0.1% Triton and 6xEDTA free protease inhibitor). After centrifugation at 2,000 g for 15 min, 1.0 mg M- and H-labeled cell lysates were mixed at a 1:1 ratio (1.0 mg total protein each) and centrifuged at 20,000 x g for 30 min at 4°C. The pellet was further processed for isolation of aggregated proteins as previously described (Tomoyasu et al., 2001). Briefly, the pellet was frozen and resuspended in 400 μL buffer A (10 mM potassium phosphate buffer, pH 6.5, 1 mM EDTA) by brief sonication. After centrifugation at 20, 000 x g for 30 min at 4°C, pellet fractions were again resuspended in 320 μL buffer A by brief sonication; afterward, 80 μL of 10% (v/v) NP40 was added. The NP40 insoluble fraction was isolated by centrifugation at 20, 000 x g for 30 min at 4°C. This washing step was repeated twice. The insoluble fraction was finally washed with 400 μL buffer A and resuspended in 100 μL buffer A. 20 μg of L-labeled cell lysate was spiked into the insoluble fraction prior to analysis by mass spectrometry.

Analysis of Thermolysin Cleaved Peptides

The thermolysin-cleaved peptides from PP treated samples (H-labeled cell culture, 100 μg) were mixed with urea (final concentration 6 M) and separated from the intact proteins in the soluble cell lysate using a filter device (Amicon Ultra-0.5 mL, Merck Millipore Ltd.) with 10 kDa cut-off at 14,000 g for 30 min. 200 μl of 8M urea was added into the filter device. After centrifugation at 14,000 g for 30 min, the filter units were washed with 200 μl of 50 mM HEPES buffer and centrifuged at 14,000 g for 15 min. This washing step was repeated twice. Filtrates were combined and fractionated with strong cation exchange (SCX) tips (Rappsilber et al., 2007). SCX StageTips were prepared by stacking 5 plugs of Empore SCX disks (Sigma-Aldrich) into a 200 μL micropipette tip as described (Rappsilber et al., 2007). Sample and washing solutions were applied to the StageTips using a centrifuge at 3,600 rpm. StageTips were consecutively washed with 100 μl of acetonitrile (ACN), and twice with 100 μl of 1% TFA. Samples were then loaded onto the StageTips and the flow-through re-loaded onto the same StageTip for another binding step. StageTips were then washed 3-times with 100 μl of 0.2% TFA. Peptides were fractionated by consecutive elution steps from SCX disks with 80 μl of 50, 100, 200, 300 and 400 mM ammonium acetate containing 20% ACN and 0.5% formic acid and a final elution step with 100 μl of 5% ammonium hydroxide/80% ACN. The elutates were dried in a vacuum centrifuge concentrator and further desalted using C18 StageTips (Rappsilber et al., 2007). C18 StageTips were prepared by stacking three punch-outs of C18 Empore Disks (Sigma-Aldrich) into a 200 μl

micropipette tip. The C18 StageTips were washed with 20 μl of ACN and centrifuged at 1,200 rpm. This washing step was repeated twice. The C18 StageTips were then washed with 20 μl of 0.1% TFA and centrifuged at 1,200 rpm. This washing step was repeated 3-times. The samples were then loaded onto the C18 StageTips and centrifuged at 1,000 rpm. The flow-through was again loaded onto the same C18 StageTip and centrifuged at 1,000 rpm. The C18 StageTips were washed with 20 μl of 0.1% TFA and centrifuged at 1,200 rpm. This washing step was repeated twice. Peptides were eluted from the StageTips with 40 μl of 0.1% formic acid/80% ACN by centrifugation at 1,200 rpm and dried in a vacuum centrifuge concentrator.

SDS-PAGE and In-gel Digestion with Trypsin

Protein mixtures were separated by SDS-PAGE on 4%–12% Bis-Tris acrylamide NuPAGE gels in MOPS SDS running buffer (Invitrogen) and stained with Coomassie Brilliant Blue. After destaining, entire gel lanes were cut into 12 (mixed cell lysates) or 4 (FLuc) slices of equal size followed by in-gel digestion. Briefly, the 12 gel slices were further cut into ~1 mm^3 cubes using a scalpel. After washing with 1 mL 50 mM ammonium bicarbonate (ABC), gel pieces were dehydrated with 1 mL ACN. After removing and discarding the supernatant, gel pieces were dried in a vacuum centrifuge concentrator for 3 min. Dehydrated gel pieces were reduced with 100 μL of 10 mM dithiothreitol in 50 mM ABC for 45 min at 56°C, and then alkylated with 100 μL of 55 mM iodoacetamide in 50 mM ABC for 30 min at room temperature in the dark. After washing with 1 mL 50 mM ABC and dehydration with ACN (1 mL), gel pieces were rehydrated in 100 μL of 50 mM ABC solution containing 15 ng/μL trypsin (sequencing grade, modified, Roche) and incubated overnight at 37°C. Peptides were extracted from gel pieces once with 750 μL of 5% formic acid/30% ACN and once with 300 μL ACN. After drying in a vacuum centrifuge concentrator, the samples were dissolved in 20 μl of 0.1% TFA and desalted with C18 StageTips as described above.

Sample Preparation for Analysis of Total Proteome and Protein Aggregates

To determine abundance fold-changes of selected protein groups (see Tables S2D, S3A, and S4C) and for the analysis of protein aggregates (see Table S2E), the Filter Aided Sample Pre (FASP) method was used to generate peptides for LC-MS/MS analysis (Wiśniewski et al., 2009). Briefly, cell lysates or aggregate fractions prepared as above were mixed with 200 μl of UA buffer (8.0 M urea in 100 mM Tris-HCl pH 8.5) in a filter unit (Amicon Ultra-0.5 mL, Merck Millipore Ltd.) with 10 kDa cut-off and centrifuged at 14,000 x g for 15 min at room temperature. The concentrates were diluted in the filter units with 200 μl of UA buffer and centrifuged again. The concentrates were incubated with 200 μl of 20 mM DTT at room temperature for 45 min. After centrifugation as above, the concentrates were alkylated in the dark for 30 min by adding 200 μl of 50 mM iodoacetamide in UA buffer. After centrifugation at 14,000 x g for 15 min, the filter units were washed with 200 μl of UA buffer and centrifuged at 14,000 x g for 15 min. This washing step was repeated twice. The filter units were then washed with 200 μl of 50 mM Tris-HCl pH 8.5 and centrifuged at 14,000 x g for 15 min. This washing step was again repeated twice. Proteins in the filter units were digested overnight in 100 μl of 50 mM Tris-HCl pH 8.5 containing 15 ng/μL trypsin. After incubation in a wet chamber at 37°C overnight, the digested peptides were collected in new tubes by centrifugation of the filter units at 14,000 x g for 10 min. 50 μl of 50 mM Tris-HCl was added in the filter units and centrifuged again. The flow-through fractions were combined and acidified with 25% trifluoroacetic acid (TFA) to a final TFA concentration of 0.1%. Tryptic peptides generated from protein aggregates were further fractionated by SCX as described above. The samples were desalted using C18 StageTips as described above, dried and resuspended in 10 μl of 5% formic acid for LC-MS/MS analysis.

Mass Spectrometry

The digested peptides were dissolved in 10 μL of 5.0% formic acid. Mass spectrometry was performed on a Q-Exactive mass spectrometer with a nanospray ion source and a nanoHPLC Proxeon EASY-nLC 1000 system (Thermo, San Jose, CA, USA). Reversed-phase separation was accomplished using a C18 AQ phase (1.9 μm, Dr. Maisch) packed silica capillary (75 μm i.d. × 250 mm length). 0.1% formic acid in H_2O was used as the mobile phase A, and 0.1% formic acid in ACN was used as the mobile phase B. About 3 μL of peptide solution was loaded onto the C18 packed capillary column and separated with a linear gradient from 5 to 35% buffer B in 120 min at a flow rate of 250 nL/min. The Q-Exactive was operated in data-dependent mode with survey scans acquired at a mass range from 300 to 1750 m/z and a resolution setting of 70,000 (FWHM). Up to ten of the most abundant ions from the survey scan were selected and fragmented by higher energy collisional dissociation. MS/MS spectra were acquired with a resolution of 17,500 (FWHM), maximum injection time of 120 ms, precursor isolation width of 2 Da, and a target value of $2e^5$.

Database Search

The acquired mass spectrometric raw data were processed using MaxQuant version 1.5.0.25 (https://www.maxquant.org/). MS/MS spectra were searched against *E. coli* K12 proteins in UniProt (version 2011-03-02). As search parameters, trypsin allowing for cleavage N-terminal to proline was chosen as enzyme specificity; Arg6, Lys4 were selected for medium-labels and Arg10, Lys8 for heavy labels; cysteine carbamidomethyl (C) was set as fixed modifications, while protein N-terminal acetylation and methionine oxidation were selected as variable modifications. A maximum of two missed cleavages and three labels were allowed. For direct identification of thermolysin-degraded peptides, mass spectrometric raw files were searched with the following parameters: Non-specific enzyme

restriction and cysteine carbamidomethyl (C) were set as fixed modifications, while protein N-terminal acetylation, methionine oxidation and heavy SILAC labeled arginine or lysine (+10 Da or +8 Da) were selected as variable modifications. In addition, semi-thermolysin-semi-tryptic peptides from in-gel digested gel slices were identified with the same parameters, except that fully tryptic peptides were excluded. Proteins and peptides (minimal seven amino acids) were identified at a false discovery rate of 1% using a target-decoy approach with a reversed database. The "re-quantify" option was enabled for protein quantification. The cleaved fraction of firefly luciferase by PP was quantified by the label free algorithm in MaxQuant.

Cutoff Control Experiment

In order to determine an appropriate cutoff value for significantly degraded proteins, we performed a control experiment in triplicate. Light and heavy labeled samples were both submitted to heat stress and were treated by pulse proteolysis under identical conditions. Then, samples were mixed and analyzed by LC-MS/MS as described above. Less than 1% of proteins had H/L ratios below 0.61 in 2 out of 3 of the control experiments. Thus, a H/L ratio of < 0.61 ($> 39\%$ of a specific protein degraded) in the PP-SILAC experiment would indicate that a protein is protease-sensitive with a statistical significance of $p < 0.01$.

Protein synthesis in exponentially growing *E. coli* (doubling time ~30 min) occurs at a rate of ~20 amino acids per second (Balchin et al., 2016). This means that an average *E. coli* protein of 310 amino acids takes about ~15 s for synthesis. We can calculate that the steady state concentration of newly synthesized (presumably not yet folded) protein is ~0.8% of total. This would likely be less in spheroplasts. The sensitivity of the PP-SILAC is such that > 39% of a protein must be degraded for that protein to be classified as protease-sensitive. Thus, our data reflect the conformational property of preexistent proteins.

Data Processing

Unless stated otherwise, protein SILAC ratios were determined from the gel-slices in which the protein was identified in highest abundance in the SILAC state without pulse proteolysis (full-length protein). Outer membrane proteins and periplasmic proteins were excluded from further analysis, because these proteins were removed during the preparation of spheroplast. Combined intensity ratios of peptides were calculated by dividing the summed intensities of heavy isotope labeled peptides from the entire gel by the summed intensities of corresponding light isotope labeled peptides. Proteins with a SILAC ratio of < 0.61 under normal condition were defined as protease-sensitive (PS). Thermo-sensitive (TS) proteins were considered as the proteins with a SILAC ratio < 0.61 that were significantly destabilized under heat stress compared to normal conditions as determined using a Student's t test in the Perseus software v.1.5.0.9 (Tyanova et al., 2016) at FDR of 0.05; the s0 value used in the global score calculation was 0.5 corresponding to a minimal fold-change of 1.5. Proteins stabilized or destabilized in KJE and ΔKJ cells were defined in the same way as described for TS proteins in WT. SILAC ratios of tryptic peptides under NC and HS conditions were also compared using Student's t test in the Perseus software at FDR of 0.05, the s0 value used in the global score calculation was 0.1. If both, the combined (entire gel) intensity and SILAC ratio of a specific tryptic peptide was lower than 0.61, then the overlapping thermolysin-degraded peptide was considered as cleavage region and used for assignment of protease-sensitive protein structures. The cleaved fraction of each protein was calculated as 1 – SILAC ratio (full-length protein). Degraded fractions of PS proteins mass was calculated:

$$\sum\{(1 - SILAC\ ratio) \times iBAQ(PS) \times Mw\} \Big/ \sum(iBAQ \times Mw)$$

The amount of mass aggregates upon heat stress was calculated:

$$\sum\{(iBAQ(H) - iBAQ(M)) \times Mw\} \times 100 \Big/ \sum(iBAQ(L) \times Mw \times 50)$$

The insoluble fraction of each protein upon heat stress was calculated:

$$\{iBAQ(H) - iBAQ(M)\} \times 100 / \ (iBAQ(L) \times 50)$$

QUANTIFICATION AND STATISTICAL ANALYSIS

Bioinformatic Analysis

Protein fold assignment was performed using SUPERFAMILY (http://supfam.org/SUPERFAMILY/downloads.html) according to the SCOP: Structural Classification of Proteins and ASTRAL. Release 1.75 classification (https://scop.berkeley.edu/astral/ver=1.75). Protein subcellular location, average hydropathy (GRAVY) of protein and peptide sequences and theoretical isoelectric points (pI) and potential DnaK binding sites were determined as described previously (Calloni et al., 2012). Gene Ontology (GO) term enrichment analysis was performed relative to all quantified proteins using the DAVID algorithm (Huang et al., 2009). A Benjamini-corrected modified Fisher's exact test was performed to examine the significance of gene-term enrichment (p value < 0.05). Protein-protein interaction network data of *E. coli* was analyzed as published (Wuchty and Uetz, 2014).

Mann-Whitney (boxplot) and chi-square χ^2 statistical significance tests (bar graphs) were performed in R (www.r-project.org). *p* value estimations for protease sensitivities in wild-type cells are based on control cutoff experiments (see "Cutoff control experiment"), whereas median p values for destabilized and stabilized proteins in KJE cells were calculated by Student's t test in Perseus v.1.5.0.9 (Tyanova et al., 2016).

DATA AND CODE AVAILABILITY

Mass spectrometry raw data have been deposited to the ProteomeXchange Consortium via PRIDE partner repository (https://www.ebi.ac.uk/pride/archive/) with the identifier PXD012929.